3) PRELIMINARY DATA

3.1 – Structure of Rep68 in complex with ITR in the apo state. We have purified the complex of Rep68 bound to a 165-nucleotide region encompassing the 3'-ITR (Figure 1A). The complex was purified to homogeneity and used to prepare grids for Cryo-EM studies. After, several rounds of screening to optimize the conditions, we collected a data set on a Titan krios microscope and generated a cryo-EM map at 6.9 Å resolution (Figure 1C). Rep68 forms a heptameric complex with ITR. The HD ring is located upstream of three OBDs bound to the RBS. The ITR three-way junction folds in such a way that hairpin1 aligns coaxially with the longer dsDNA region and hairpin2 protrudes antiparallel them (Figure 1D). This conformation of the ITR is supported by previous computational and NMR studies of three-way DNA junctions. Our Cryo-EM structure supports the model where the hairpin2 tip, with three unpaired thymines bind the ssDNA binding site of one of the OBDs bound to the RBS (Figure 1E).

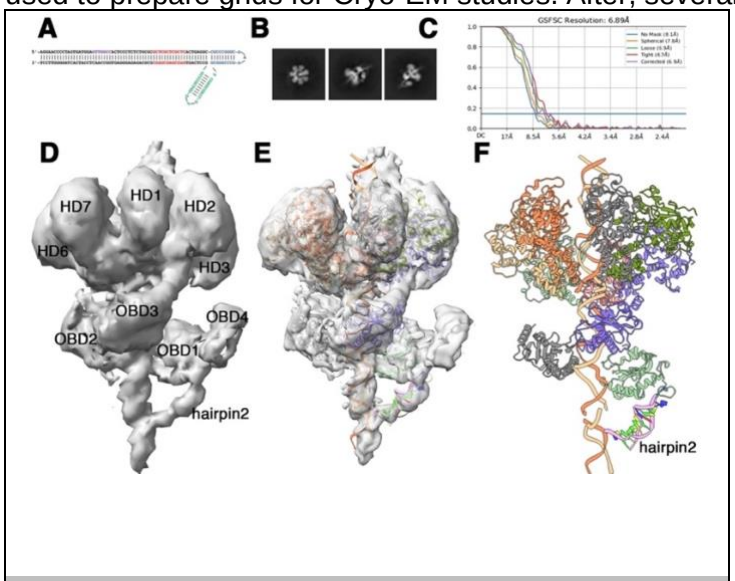

Figure 1. Cryo-EM Structure Rep68-ITR-apo. (A) ITR sequence used in complex formation. The diagram shows hairpin1 (blue) coaligned with the main sequence. In red is RBS. Green section is hairpin2. (B) Sample of representative of 2D classes. (C) Gold standard FSC calculated in cryosparc. (D) Cryo-EM map of the complex; Rep domains are labelled. (E) Partial model of the complex fitted to the density includes seven helicase domains and three OBDs. Full sequence of hairpin2 is shown in pink, although connections to main ITR cannot be made at this time. (F) Ribbon representation of the complex.

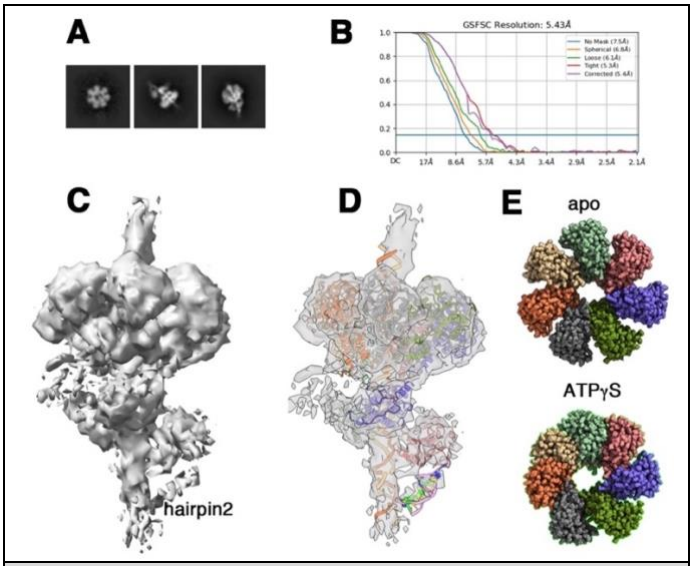

Figure 2. Cry-EM structure of the Rep68-ITR/ATPγS complex. (A) Representative 2D classes of selected particles. (B) Gold Standard FSC curve using cryosparc. (C) Cryo-EM map of the complex. (D) Fitted model of heptameric HD and three OBDs. (E) Comparison of conformation changes in the HD upon binding ATPγS.

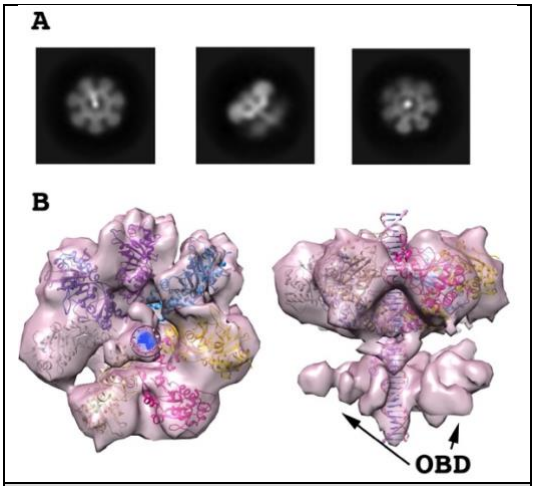

Figure 3. Cryo-EM of Rep68-dsAAVS1 complex. (A) representative 2D averages of the complex. (B) two orthogonal views of the heptameric complex with seven docked helicase domains. The density of most of the 41-bp AAVS1 site can be seen in the map and shows curvature at different sites (C).

3.2 Determine the cryo-EM structure of the Rep68-ITR complex with ATPγS. We have determined the structure of the Rep68-ITR complex to an overall resolution of 5.4 Å. The complex remains heptameric, but the HD subunits are closer to compared to the apo structure (Figure 2). Three of the subunits interact with DNA through the PS1βH region, similarly to the AAVS1 complex. The three OBD molecules are still bound to the RBS site, although the densities are less defined when compared to the apo complex. We can discern that there are changes in the region of the hairpin2, but resolution is not sufficient to see any details of the interactions.

3.3 Determine the cryo-EM structure of Rep68-AAVS1 in ATPγS bound state. We have now determined the structure of the Rep68-dsAAVS1 in the presence of ATPγS to 5.8 Å (Figure 3). This resolution is a significant improvement from the apo complex and suggests that higher resolution structures of these complexes are feasible. We observed that the density of the hairpin2 region is less defined as compared to the apo structure and may represent dynamic states. Also observed in this map is a widening in the DNA groves in the RBS region. There is also a small

reorientation of the OBD bound to hairpin2. The collection of additional data will be needed to observe all the changes associated with ATP binding.

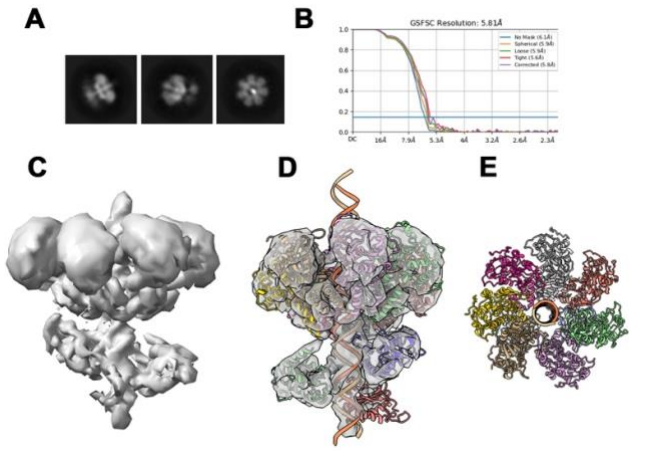

Figure 4. Cryo-EM structure Rep68-dsAAVS1/ATPγS. (A) Representative 2D classes. (B) Gold Standard FSC after non-uniform refinement in cryosparc. (C) Cryo-EM map of complex. (D) Seven helicase domains and three OBDs where fitted to the density along with a 50-bp AAVS1 site. (E) Top view of helicase ring showing the seven subunits.

3.4 ***Structure of Rep68-dsAAVS1-apo state.*** We determined a preliminary cryo-EM structure of the apo complex to ~9 Å resolution (Figure 3). Preliminary structure shows: 1) We were able to confirm that the complex is heptameric although very asymmetric; 2) The helicase domains have better density than the OBDs; 3) Only four of the HDs have full densities; 4) The OBDs are also engaged with the DNA and probably interacting with the GCTC repeats; 5) There is significant deformation in the dsDNA molecule.

3.5 Structure of Rep68-dsAAVS1-ATPγS. We determined the structure of Rep68 bound to the AAVS1 site in presence of ATPγS to an overall resolution of 5Å (Figure 4).

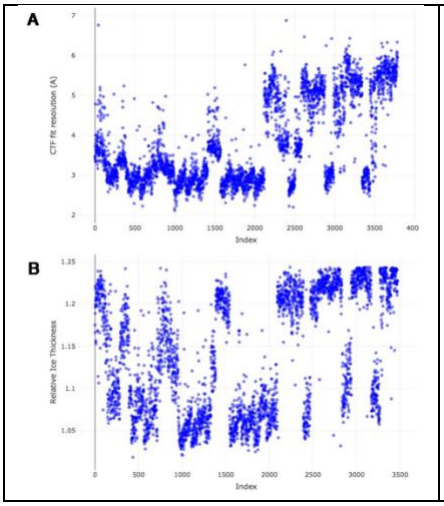

Figure 5. Comparison of CTF fit resolution and ice thickness of micrographs.
(A) Plot of CTF fit resolution and Index number and (B) ice thickness and index number. Regions of better CTF fit correlate with thinner ice regions.